A spatial sixth-order alternating direction implicit method for two-dimensional cubic nonlinear Schrödinger equations ☆

Leonard Z. Li[1], Hai-Wei Sun[1,*], Sik-Chung Tam[1]

Department of Mathematics, University of Macau, Macao

Abstract

Based on the combined compact difference scheme, an alternating direction implicit method is proposed for solving two-dimensional cubic nonlinear Schrödinger equations. The proposed method is sixth-order accurate in space and second-order accurate in time. The linear Fourier analysis method is exploited to study the stability of the proposed method. The efficiency and accuracy of the proposed method are tested numerically, and the common solution pattern of the nonlinear Schrödinger equation is also illustrated using relevant examples known in the literature.

Keywords: Cubic nonlinear Schrödinger equation, combined compact difference scheme, alternating direction implicit method, unconditional stability, solution pattern, wave-like motion

1. Introduction

In this paper, we study the following two-dimensional cubic nonlinear Schrödinger equation (NLSE),

$$\mathbf{i}\frac{\partial u}{\partial t} + a\frac{\partial^2 u}{\partial x^2} + b\frac{\partial^2 u}{\partial y^2} + q|u|^2 u + v(x,y)u = 0,\ (x,y,t) \in \Omega \times (0,T], \tag{1}$$

accompanied with the following initial condition

$$u(x,y,0) = u_0(x,y),\ (x,y) \in \Omega, \tag{2}$$

and the Dirichlet boundary condition

$$u(x,y,t) = g(x,y,t),\ (x,y) \in \partial\Omega,\ t \in (0,T], \tag{3}$$

☆The research was partially supported by the research grant 005/2012/A1 from FDCT of Macao, and MYRG206 (Y3-L4)-FST11-SHW, from University of Macau.

*Corresponding author

Email addresses: reachless@live.cn (Leonard Z. Li), HSun@umac.mo (Hai-Wei Sun), fstsct@umac.mo (Sik-Chung Tam)

within the rectangular domain $\Omega = [L_x, R_x] \times [L_y, R_y] \in \mathbb{R}^2$ and computational time interval $(0, T]$, where $\mathbf{i} \equiv \sqrt{-1}$ is the complex unit, $a,\ b$, and q are real constants, $\partial\Omega$ is the boundary of Ω, u_0 and g are given sufficiently smooth functions, v is an arbitrary real-valued potential function, and $u(x, y, t)$ is an unknown complex-valued wave function which describes the motion of soliton(s) [5].

The NLSE is one of the most important equations of mathematical physics and it has been widely used to model various nonlinear physical phenomena, such as underwater acoustics, quantum mechanics, plasma physics, bimolecular dynamics, nonlinear optics, and electromagnetic wave propagation [15]. The cubic NLSE is one of the most important topics of the NLSE, and is also known as Gross-Pitaevskii equation (GPE) which plays a fundamental role in modeling the hydrodynamics of Bose-Einstein condensate [12, 14, 9, 2, 3, 27, 28, 1].

Recently, due to the wide use of the NLSE, numerous researchers show intensive interest in developing numerical methods to solve this kind of equation, including finite difference methods [25, 16, 8]. The alternating direction implicit (ADI) method, which was first proposed by Peaceman and Rachford [18], and hereafter referred to as PRADI, is one of the involved methods, and famous for its high efficiency. The ADI method turns the original multi-dimensional problem into a collection of one-dimensional problems, which generally only requires the handle of tridiagonal systems, thus leads to its good reputation of high efficiency. Nevertheless, the spatially second-order accuracy of the original ADI method limits its application in more and more challenging computational problems. To increase the spatial accuracy of the ADI method, one way is to exploit the higher order compact (HOC) difference schemes [13, 22, 21], which have been widely utilized due to their higher-order accuracies while no extra difficulty is posed comparing with the conventional difference schemes. In [11], based on the standard fourth-order Padé scheme, Gao and Xie developed an ADI method, which is fourth-order accurate in space and second-order accurate in time, to solve two-dimensional Schrödinger equations. Lately, Xu and Zhang [26] proposed a spatially fourth-order and temporally second-order accurate HOC-ADI method to solve the two-dimensional cubic NLSE. In [2, 1], the authors compared and reviewed different numerical methods for solving NLSE/GPE.

The combined compact difference (CCD) scheme, first proposed by Chu and Fan [7] in 1998, was intended to solve one-dimensional or two-dimensional steady convection-diffusion equations. The three-point sixth-order CCD method is an implicit scheme with a triple-tridiagonal matrix as its coefficient matrix, which can be solved with triple-forward elimination and triple-backward substitution [7]. When the CCD scheme is applied to solve an equation, we do not discretize the first and second derivatives in the original equation, but use two appropriate formulae to approximate them respectively. Hence the unknown variable in the equation is solved jointly with its first and second derivatives in a triple-tridiagonal system. Actually, this distinguishing feature, renders the CCD scheme especially suitable for solving nonlinear equations as well as the equations with variable coefficients. Since equation (1) is a nonlinear equation, it is reasonable for us to take advantage of the CCD scheme to solve it.

A CCD-ADI method [19] is proposed for the two-dimensional unsteady convection-

diffusion equation, by combining the CCD scheme and the ADI method together. The CCD-ADI method is a D'Yakonov ADI-like scheme, which requires one to determine the boundary condition of the intermediate variable based on the second equation of the CCD-ADI method in a complicated way, including an extra step to calculate the partial derivatives with respect to y deliberately. Though the handling of the intermediate boundary condition of the D'Yakonov ADI-like scheme improves accuracy, it extends the computational time significantly.

In this paper, we develop a CCD-PRADI method by employing the CCD and ADI method to solve the two-dimensional cubic NLSE. To circumvent the inconvenience in determining the boundary condition of the intermediate variable, we exploit the PRADI scheme in the derivation of the CCD-PRADI method; we also simply take the intermediate boundary condition by calculating the Dirichlet boundary condition (3) in the implementation. Although it is not encouraged to take the intermediate boundary condition by this manner in many literatures [10], such a seemingly clumsy handling turns out to be effective and satisfactory, due to the high accuracy of the CCD method. In the first step of the derivation of our CCD-PRADI method, we discretize the original equation temporally with the Crank-Nicolson scheme and then factorize the resulting semi-discretization into the PRADI scheme with two one-dimensional problems. In the second step, the CCD method is exploited to solve the two one-dimensional problems with the efficient triple-forward elimination and triple-backward substitution. An elaborate algorithm is proposed to guide the implementation of the CCD-PRADI method for solving the two-dimensional cubic NLSE. The CCD-PRADI method is sixth-order accurate in space and second-order accurate in time. If the constants a, b, and q are not too big, i.e., equation (1) without singularity, then, as in [6], we can employ the linear Fourier analysis method [26, 5, 4] to study the stability of the proposed method.

The rest of this paper is organized as follows. In section 2, we propose a CCD-PRADI method for the two-dimensional cubic NLSE. The linear stability analysis for the proposed CCD-PRADI method is studied in section 3. Section 4 contains some numerical examples to show the performance of the proposed method, as well as the common solution pattern of the NLSE. Some remarks on the proposed method are further elaborated in the last section.

2. CCD-PRADI method for the cubic NLSE

In this section, we first discretize equation (1) temporally and then apply the CCD scheme to obtain the full discretization to give rise to the CCD-PRADI method for the cubic NLSE. Due to the nonlinearity of (1), the CCD-PRADI method requires an iterative process for each unknown time level to produce an approximate solution.

For convenience, we rewrite equation (1) as the following form

$$\frac{\partial u}{\partial t} - \mathbf{i}a\frac{\partial^2 u}{\partial x^2} - \mathbf{i}b\frac{\partial^2 u}{\partial y^2} - \mathbf{i}q|u|^2 u - \mathbf{i}v(x,y)u = 0. \tag{4}$$

In the first place, we divide the time interval $[0, T]$ into N equally sub-intervals, with the time step $\Delta t = T/N$ and $t_n = n\Delta t$, $n = 0, 1, \ldots, N$. Let ϕ^α be the approximation of

$\phi(x,y,\alpha\Delta t)$ for an arbitrary function $\phi(x,y,t)$ with positive real number α. Applying the Crank-Nicolson scheme to discretize the temporal derivative in (4) around $t=t_n+\frac{1}{2}\Delta t$, we have

$$\begin{aligned}\frac{u^{n+1}-u^n}{\Delta t} &= \mathbf{i}a\frac{\frac{\partial^2 u^{n+1}}{\partial x^2}+\frac{\partial^2 u^n}{\partial x^2}}{2}+\mathbf{i}b\frac{\frac{\partial^2 u^{n+1}}{\partial y^2}+\frac{\partial^2 u^n}{\partial y^2}}{2}\\ &\quad +\mathbf{i}q\frac{|u^{n+1}|^2u^{n+1}+|u^n|^2u^n}{2}+\mathbf{i}v\frac{u^{n+1}+u^n}{2}+\mathcal{O}(\Delta t^2).\end{aligned}$$

Note that $\phi^{n+\frac{1}{2}}=\dfrac{\phi^{n+1}+\phi^n}{2}+\mathcal{O}(\Delta t^2)$, we obtain following equation which is equivalent to the above one,

$$\begin{aligned}\frac{u^{n+1}-u^n}{\Delta t} &= \mathbf{i}a\frac{\partial^2 u^{n+\frac{1}{2}}}{\partial x^2}+\mathbf{i}b\frac{\frac{\partial^2 u^{n+1}}{\partial y^2}+\frac{\partial^2 u^n}{\partial y^2}}{2}\\ &\quad +\mathbf{i}q\frac{|u^{n+1}|^2u^{n+1}+|u^n|^2u^n}{2}+\mathbf{i}vu^{n+\frac{1}{2}}+\mathcal{O}(\Delta t^2).\end{aligned}\tag{5}$$

Since the coefficients a, b and q are constants, we can apply the PRADI scheme [18] to solve the above equation. We first solve $\frac{\partial^2 u}{\partial x^2}$ on the intermediate layer $t=t_n+\frac{1}{2}\Delta t$ with $\frac{\partial^2 u}{\partial y^2}$ given on the n-th time level, and then solve $\frac{\partial^2 u}{\partial y^2}$ on the $(n+1)$-st time level with the just computed $\frac{\partial^2 u}{\partial x^2}$ on the intermediate layer. Finally we obtain the following PRADI scheme

$$\begin{cases} u^{n+\frac{1}{2}}\left[1-\mathbf{i}\dfrac{\Delta t}{2}v\right]-\mathbf{i}\dfrac{a\Delta t}{2}\dfrac{\partial^2 u^{n+\frac{1}{2}}}{\partial x^2}=\mathbf{i}\dfrac{b\Delta t}{2}\dfrac{\partial^2 u^n}{\partial y^2}+u^n\left[1+\mathbf{i}\dfrac{q\Delta t}{2}|u^n|^2\right], & (6)\\ u^{n+1}\left[1-\mathbf{i}\dfrac{q\Delta t}{2}|u^{n+1}|^2\right]-\mathbf{i}\dfrac{b\Delta t}{2}\dfrac{\partial^2 u^{n+1}}{\partial y^2}=\mathbf{i}\dfrac{a\Delta t}{2}\dfrac{\partial^2 u^{n+\frac{1}{2}}}{\partial x^2}+u^{n+\frac{1}{2}}\left[1+\mathbf{i}\dfrac{\Delta t}{2}v\right]. & (7)\end{cases}$$

In the above ADI scheme (6) and (7), we put the nonlinear term and $\frac{\partial^2 u}{\partial y^2}$ together, thus we have to solve a nonlinear equation (7), which is generally solved by time consuming iteration. However, comparing with the HOC-ADI method proposed in [26], the above PRADI scheme has a remarkable improvement, that is only one equation, equation (7), is required to be solved iteratively. Nevertheless, in the implementation of the HOC-ADI method [26], one is required to solve two equations in each iteration, in other words, the HOC-ADI method needs to solve two equations iteratively. Therefore, we can infer that such arrangement in the above PRADI scheme will improve the efficiency.

Up to now, we have only obtained the temporal discretization of (4). In order to carry out the spatial discretization, we divide the domain Ω into a uniform grid denoted by the grid set $\{(x_j,y_k)\}$, in which $x_j=L_x+j\Delta x$ and $y_k=L_y+k\Delta y$, where $j=0,1,\ldots,M_x$ and $k=0,1,\ldots,M_y$, Δx and Δy are grid steps, and M_x and M_y are grid numbers in x- and y-directions, respectively.

Let $\phi^t_{j,k}$ be an approximation of $\phi(x_j,y_k,t)$ for an arbitrary function $\phi(x,y,t)$. Based on the PRADI scheme (6) and (7), an implementable computational scheme to solve (4) is

yielded, by employing arbitrary difference scheme that approximates the second derivative, for instance, the central difference scheme and the standard fourth-order Padé scheme. Note that both equations (6) and (7) are one-dimensional problems, as well as the outstanding applicability of the CCD method in solving nonlinear equations, hence we can take advantage of the following sixth-order CCD scheme [7, 19] to solve (6) and (7),

$$\frac{7}{16}(\varphi'_{i+1}+\varphi'_{i-1})+\varphi'_i-\frac{h}{16}(\varphi''_{i+1}-\varphi''_{i-1})-\frac{15}{16h}(\varphi_{i+1}-\varphi_{i-1})=0 \tag{8}$$

and

$$\frac{9}{8h}(\varphi'_{i+1}-\varphi'_{i-1})+\varphi''_i-\frac{1}{8}(\varphi''_{i+1}+\varphi''_{i-1})+\frac{3}{h^2}(\varphi_{i+1}-2\varphi_i+\varphi_{i-1})=0, \tag{9}$$

where h is the grid size in space, φ is an arbitrary sufficiently smooth function, and $\varphi'_i \approx \varphi'(\nu_i)$, $\varphi''_i \approx \varphi''(\nu_i)$, ν_i is either x_j or y_k in the above uniform grid.

Let $(u_{xx})^t_{j,k} \approx \frac{\partial^2 u(t)}{\partial x^2}|_{(x_j,y_k)}$ and $(u_{yy})^t_{j,k} \approx \frac{\partial^2 u(t)}{\partial y^2}|_{(x_j,y_k)}$ at any time t, then the CCD-PRADI scheme is presented as follows,

$$\begin{cases} u^{n+\frac{1}{2}}_{j,k}\left[1-\mathbf{i}\frac{\Delta t}{2}v_{j,k}\right]-\mathbf{i}\frac{a\Delta t}{2}(u_{xx})^{n+\frac{1}{2}}_{j,k}=\mathbf{i}\frac{b\Delta t}{2}(u_{yy})^n_{j,k}+u^n_{j,k}\left[1+\mathbf{i}\frac{q\Delta t}{2}|u^n_{j,k}|^2\right], & (10)\\ u^{n+1}_{j,k}\left[1-\mathbf{i}\frac{q\Delta t}{2}|u^{n+1}_{j,k}|^2\right]-\mathbf{i}\frac{b\Delta t}{2}(u_{yy})^{n+1}_{j,k}=\mathbf{i}\frac{a\Delta t}{2}(u_{xx})^{n+\frac{1}{2}}_{j,k}+u^{n+\frac{1}{2}}_{j,k}\left[1+\mathbf{i}\frac{\Delta t}{2}v_{j,k}\right], & (11)\end{cases}$$

where the second partial derivatives in (10) and (11) are approximated by (9).

As mentioned before, the boundary value of the intermediate variable $u^{n+\frac{1}{2}}_{j,k}$ for $j=0,\ M_x$ and $k=0,\ 1,\ldots,\ M_y$ in (10) is directly taken from the boundary condition (3). This is actually a much more efficient way to determine the boundary value of the intermediate variable than that of the CCD-ADI method proposed in [19]. The CCD-ADI method is a D'Yakonov ADI-like scheme, which requires to determine the boundary value of the intermediate variable by the second equation of the CCD-ADI scheme based on the boundary value of u^{n+1}. This incurs an extra step in the implementation of the CCD-ADI method to determine the boundary condition of the intermediate variable, by first computing the first and second partial derivatives with respect to y by the CCD method. Though such a handling of the intermediate boundary value indeed improves the accuracy of the intermediate boundary value, it significantly increases the computational time. Most importantly it is no longer critical when a spatially higher-order accurate method, such as the CCD method, is exploited with the ADI method. On the other hand, in the CCD-PRADI scheme (10) and (11), we can obtain the satisfactory boundary condition of $u^{n+\frac{1}{2}}_{j,k}$ by simply computing (3). From the numerical results in section 4, we conclude that the CCD-PRADI scheme (10) and (11) is a satisfactory method, which also indicate the validity in determining the intermediate boundary condition of the proposed CCD-PRADI method.

In the implementation of the CCD-PRADI method, we have the above CCD formulae (8) and (9) associated with (10) or (11), to form a system, which is usually not closed in the

boundary. To close the system, we have to further exploit the following fifth-order one-sided boundary conditions [7, 19],

$$14\varphi_0' + 16u_1' + 2h\varphi_0'' - 4h\varphi_1'' + \frac{1}{h}(31\varphi_0 - 32\varphi_1 + \varphi_2) = 0 \tag{12}$$

and

$$14\varphi_M' + 16\varphi_{M-1}' - 2h\varphi_M'' + 4h\varphi_{M-1}'' - \frac{1}{h}(31\varphi_M - 32\varphi_{M-1} + \varphi_{M-2}) = 0, \tag{13}$$

where M is either M_x or M_y. Moreover, it is also worth noting that although we employ the fifth-order boundary conditions (12) and (13), the sixth-order accuracy of the CCD method is attainable, which can be confirmed in numerical results as in [7, 19, 20]. Therefore, we assert that the CCD-PRADI method is theoretically and numerically sixth-order accurate in space.

To initiate the computation, we first need to compute $(u_{yy})_{j,k}^0$ with a high-order accurate method with initial value $u_0(x, y)$, which can be accomplished by the CCD method. Nevertheless, besides the CCD formulae (8)–(9) and (12)–(13), we need the following two additional boundary conditions [19],

$$\varphi_0' + 2\varphi_1' - h\varphi_1'' = -\frac{1}{2h}(7\varphi_0 - 8\varphi_1 + \varphi_2) \tag{14}$$

and

$$\varphi_M' + 2\varphi_{M-1}' + h\varphi_{M-1}'' = \frac{1}{2h}(7\varphi_M - 8\varphi_{M-1} + \varphi_{M-2}), \tag{15}$$

to close the system for derivative calculation.

Generally, the coefficient $q \neq 0$, hence (11) is a nonlinear equation since the coefficient $\mathbf{i}\frac{q\Delta t}{2}|u_{j,k}^{n+1}|^2 \neq 0$. Thus the Picard iteration, which is also called fixed-point iteration, is exploited to solve (11), yielding the following iterative process in the implementation of the CCD-PRADI scheme,

$$\begin{cases} u_{j,k}^{n+\frac{1}{2}}\left(1 - \mathbf{i}\dfrac{\Delta t}{2}v_{j,k}\right) - \mathbf{i}\dfrac{a\Delta t}{2}(u_{xx})_{j,k}^{n+\frac{1}{2}} = \mathbf{i}\dfrac{b\Delta t}{2}(u_{yy})_{j,k}^{n} + u_{j,k}^{n}\left(1 + \mathbf{i}\dfrac{q\Delta t}{2}|u_{j,k}^{n}|^2\right), \\ (u_{j,k}^{n+1})^*\left[1 - \mathbf{i}\dfrac{q\Delta t}{2}|(u_{j,k}^{n+1})_s|^2\right] - \mathbf{i}\dfrac{b\Delta t}{2}(u_{yy})_{j,k}^{*} = \mathbf{i}\dfrac{a\Delta t}{2}(u_{xx})_{j,k}^{n+\frac{1}{2}} + u_{j,k}^{n+\frac{1}{2}}\left(1 + \mathbf{i}\dfrac{\Delta t}{2}v_{j,k}\right), \end{cases}$$

where $(u_{j,k}^{n+1})^*$ and $(u_{yy})_{j,k}^*$ denote the $(s+1)$-st iterative solution and $(u_{j,k}^{n+1})_s$ is the s-th iterative solution to (11) for each unknown time level. The initial value for the iteration is chosen as $(u_{j,k}^{n+1})_0 = u_{j,k}^n$, and the iteration is carried out until the stopping criterion $\max|(u_{j,k}^{n+1})^* - (u_{j,k}^{n+1})_s| < 10^{-6}$ is satisfied.

We give the following algorithm to show the detailed instruction for the implementation of the CCD-PRADI method to solve Eq. (1).

Algorithm 1: Implementation of the CCD-PRADI method

1. Do $j = 0, 1, \ldots, M_x$

   Compute $(u^0_{yy})_{j,k}$ by (8)–(9), (12)–(13) and (14)–(15) for $k = 0, 1, \ldots, M_y$

2. Do $n = 0, 1, \ldots, N-1$

   (a) Compute the right-hand side of (10) for all mesh points

   and the boundary conditions $u^{n+\frac{1}{2}}_{j,k}$ for $j = 0$, M_x and $k = 0, 1, \ldots, M_y$

   i. $f^n_{j,k} := \mathbf{i}\frac{b\Delta t}{2}(u_{yy})^n_{j,k} + u^n_{j,k}\left[1 + \mathbf{i}\frac{q\Delta t}{2}|u^n_{j,k}|^2\right]$

   ii. $u^{n+\frac{1}{2}}_{j,k} := g(x_j, y_k, n\Delta t + \frac{\Delta t}{2})$

   (b) Solve (10), i.e. $u^{n+\frac{1}{2}}_{j,k}\left[1 - \mathbf{i}\frac{\Delta t}{2}v_{j,k}\right] - \mathbf{i}\frac{a\Delta t}{2}(u_{xx})^{n+\frac{1}{2}}_{j,k} = f^n_{j,k}$,

   with the CCD scheme (8)–(9), (12)–(13) and boundary conditions $u^{n+\frac{1}{2}}_{j,k}$

   (c) Compute the right-hand side of (11) for all mesh points

   $f^{n+1}_{j,k} := \mathbf{i}\frac{a\Delta t}{2}(u_{xx})^{n+\frac{1}{2}}_{j,k} + u^{n+\frac{1}{2}}_{j,k}\left[1 + \mathbf{i}\frac{\Delta t}{2}v_{j,k}\right]$

   (d) Solve (11), i.e. $(u^{n+1}_{j,k})^*\left[1 - \mathbf{i}\frac{q\Delta t}{2}|(u^{n+1}_{j,k})_s|^2\right] - \mathbf{i}\frac{b\Delta t}{2}(u_{yy})^*_{j,k} = f^{n+1}_{j,k}$

   i. Initiate the iteration with $(u^{n+1}_{j,k})_s := u^n_{j,k}$ and $eps := 1$

   ii. While $eps \geq 10^{-6}$, do

   (i). Solve $(u^{n+1}_{j,k})^*\left[1 - \mathbf{i}\frac{q\Delta t}{2}|(u^{n+1}_{j,k})_s|^2\right] - \mathbf{i}\frac{b\Delta t}{2}(u_{yy})^*_{j,k} = f^{n+1}_{j,k}$

   with the CCD scheme (8)–(9), (12)–(13) and boundary conditions $u^{n+1}_{j,k}$

   (ii). Error calculation $eps = \max|(u^{n+1}_{j,k})^* - (u^{n+1}_{j,k})_s|$

   and solution update $(u^{n+1}_{j,k})_s = (u^{n+1}_{j,k})^*$

   iii. $u^{n+1}_{j,k} = (u^{n+1}_{j,k})^*$

3. Stability analysis

We now study the stability of the CCD-PRADI method (10) and (11) for solving (1). Here, we only consider equations without singularity (where a, b, q are not too big), which allow us to study the stability using linear Fourier method; see [26, 5, 4, 6].

Assume that u is periodic in both x- and y- directions, and at grid node (j, k), let

$$u^n_{j,k} = \xi^n e^{\mathbf{i}(w_x j + w_y k)},\ (u_{xx})^n_{j,k} = \mu^n_x e^{\mathbf{i}(w_x j + w_y k)},\ (u_{yy})^n_{j,k} = \mu^n_y e^{\mathbf{i}(w_x j + w_y k)} \tag{16}$$

where ξ^n, μ^n_x, μ^n_y are amplitudes at time level n, and w_x and w_y are phase angles in x- and y-directions, respectively.

In [19], we revealed the relationship between μ^n_x, μ^n_y and ξ^n, which is concluded as the following lemma.

Lemma 1. (see [19, Lemma 1]) *The amplitudes μ^n_x, μ^n_y and ξ^n are related in the following*

formulas

$$\begin{cases} \mu_x^n = \dfrac{\xi^n C_x}{\Delta x^2 A_x}, \\ \mu_y^n = \dfrac{\xi^n C_y}{\Delta y^2 A_y}, \end{cases}$$

where $A_{x(y)} = 20\cos w_{x(y)} + 2\cos^2 w_{x(y)} + 23$ *and* $C_{x(y)} = 3(8\cos w_{x(y)} + 11\cos^2 w_{x(y)} - 19)$.

Let $\alpha_x = \dfrac{C_x}{\Delta x^2 A_x}$ and $\alpha_y = \dfrac{C_y}{\Delta y^2 A_y}$, by the above lemma, we have

$$\begin{cases} (u_{xx})_{j,k}^n = \mu_x^n e^{\mathbf{i}(w_x j + w_y k)} = \alpha_x u_{j,k}^n, \\ (u_{yy})_{j,k}^n = \mu_y^n e^{\mathbf{i}(w_x j + w_y k)} = \alpha_y u_{j,k}^n \end{cases} \tag{17}$$

For the linear Fourier analysis, as in [26, 6], we set $|u_{j,k}^n|^2 = c$, where c is constant. Then the scheme (10)–(11) can be rewritten as

$$\begin{cases} u_{j,k}^{n+\frac{1}{2}}(1 - \mathbf{i}\frac{\Delta t}{2} v_{j,k}) - \mathbf{i}\frac{a\Delta t}{2}(\frac{\partial^2 u}{\partial x^2})_{j,k}^{n+\frac{1}{2}} = \mathbf{i}\frac{b\Delta t}{2}(\frac{\partial^2 u}{\partial y^2})_{j,k}^n + u_{j,k}^n(1 + \mathbf{i}\frac{qc\Delta t}{2}), \\ u_{j,k}^{n+1}(1 - \mathbf{i}\frac{qc\Delta t}{2}) - \mathbf{i}\frac{b\Delta t}{2}(\frac{\partial^2 u}{\partial y^2})_{j,k}^{n+1} = \mathbf{i}\frac{a\Delta t}{2}(\frac{\partial^2 u}{\partial x^2})_{j,k}^{n+\frac{1}{2}} + u_{j,k}^{n+\frac{1}{2}}(1 + \mathbf{i}\frac{\Delta t}{2} v_{j,k}). \end{cases} \tag{18}$$

Substitute (16) and (17) into (18), we have

$$\begin{cases} [1 - \frac{\Delta t}{2}(v_{j,k} + a\alpha_x)\mathbf{i}] u_{j,k}^{n+\frac{1}{2}} = [1 + \frac{\Delta t}{2}(qc + b\alpha_y)\mathbf{i}] u_{j,k}^n, \\ [1 - \frac{\Delta t}{2}(qc + b\alpha_y)\mathbf{i}] u_{j,k}^{n+1} = [1 + \frac{\Delta t}{2}(v_{j,k} + a\alpha_x)\mathbf{i}] u_{j,k}^{n+\frac{1}{2}}. \end{cases}$$

Therefore, amplitude ξ for the proposed CCD-PRADI method is

$$|\xi| = \left| \frac{u_{j,k}^{n+1}}{u_{j,k}^n} \right| = \left| \frac{[1 + \frac{\Delta t}{2}(qc + b\alpha_y)\mathbf{i}][1 + \frac{\Delta t}{2}(v_{j,k} + a\alpha_x)\mathbf{i}}{[1 - \frac{\Delta t}{2}(qc + b\alpha_y)\mathbf{i}][1 - \frac{\Delta t}{2}(v_{j,k} + a\alpha_x)\mathbf{i}]} \right| = 1.$$

Therefore, it meets the unconditionally stable criterion ($|\xi| \leq 1$) and we conclude that the proposed CCD-PRADI method is unconditionally stable.

4. Numerical experiments

In this section, we test some problems and present the numerical results by the CCD-PRADI method. For comparison of high order accuracy and efficiency, we also present the numerical results by the HOC-ADI methods [26]. All experiments are performed based on Matlab 7.13 on a Dell Vostro 260s computer with 3.1 GHz Intel Core i5-2400 CPU and 4GB RAM.

Example 1.

Consider equation (1) in the domain $-2.5 \leq x, y \leq 2.5$ with coefficients $a = b = 1$, $q = 0$ and $v(x, y) = 0$. Obviously, this is a problem of non-homogeneous boundary condition, and the analytic solution is given by

$$u(x, y, t) = \frac{\mathbf{i}}{\mathbf{i} - 4t} \exp\left(- \frac{\mathbf{i}}{\mathbf{i} - 4t}(x^2 + y^2 + \mathbf{i}k_0 x + \mathbf{i}k_0^2 t)\right),$$

which is same as the case in [26]. Both the initial condition (2) and Dirichlet boundary condition (3) are directly taken from the above analytic solution, and we take the wave number k_0 as 5. This problem is a transient Gaussian distribution [26, 23] which originally centered at $(0, 0)$ and drifting to the negative x direction as time goes on. It is also worth noting that drifting is a common solution pattern of the nonlinear Schrödinger equations [17].

The CCD-PRADI method is employed to simulate this problem under a uniform grid with grid space $\Delta x = \Delta y = h = \frac{1}{40}$ and time step $\Delta t = \frac{1}{1000}$, as in [26, 23]. Fig. 1–2 show the figures of numerical solutions and absolute errors at three moments, $t = 0.25,\ 0.35,$ and 0.5 by the CCD-PRADI method and the HOC-ADI method, respectively. In view of such two figures, we conclude that the CCD-PRADI method is non-oscillating, as the HOC-ADI method [26]. Indeed, it is capable to simulate the evolution of the solution. Moreover, the absolute error at $t = 0.5$ shows that the CCD-PRADI method is more accurate than the HOC-ADI method.

Example 2.

Taking the coefficients in (1) as $a = b = \frac{1}{2},\ q = -1$, with the potential function given as $v(x, y) = -[1 - \sin^2(x)\sin^2(y)]$ in the domain $0 \leq x, y \leq 2\pi$, then the analytic solution to equation (1) is given by

$$u(x, y, t) = \sin(x)\sin(y)\exp(-\mathbf{i}2t).$$

As in *Example 1*, the initial condition and the Dirichlet boundary condition can be immediately taken as $u_0(x, y) = \sin(x)\sin(y)$ and $g(x, y, t) = 0$, respectively.

Example 2 is solved under a uniform grid ($\Delta x = \Delta y = h$) to show the spatial convergence rates of the HOC-ADI method and the present CCD-PRADI method. The numerical results are presented in Table 1 to compare their accuracies under the relative L^2-norm error of the numerical solution with respect to the analytic solution, and to show the efficiency of two methods. In all tables, "Rate" denotes the convergence rate (Rate $= \ln(err1/err2)$) of each method, where $err1$ and $err2$ are relative L^2-norm errors corresponding to the mesh sizes h and $h/2$, respectively, and "CPU" denotes the total CPU time in seconds for each method to solve the discretized system of (1).

Table 1 presents the relative L^2-norm errors of the approximations with respect to the analytic solution and spatial convergence rates of these two methods. In the computation, we fix the time step $\Delta t = \frac{1}{5000}$ and final time $T = 1$ to validate the spatial accuracy. From the results shown in the Table 1, we can conclude that the present CCD-PRADI method is much more accurate than the HOC-ADI method. Moreover, when the mesh size is $\Delta x = \Delta y = \frac{\pi}{8}$, the error of the CCD-PRADI method is 4.3040×10^{-6} and the CPU time consumed is

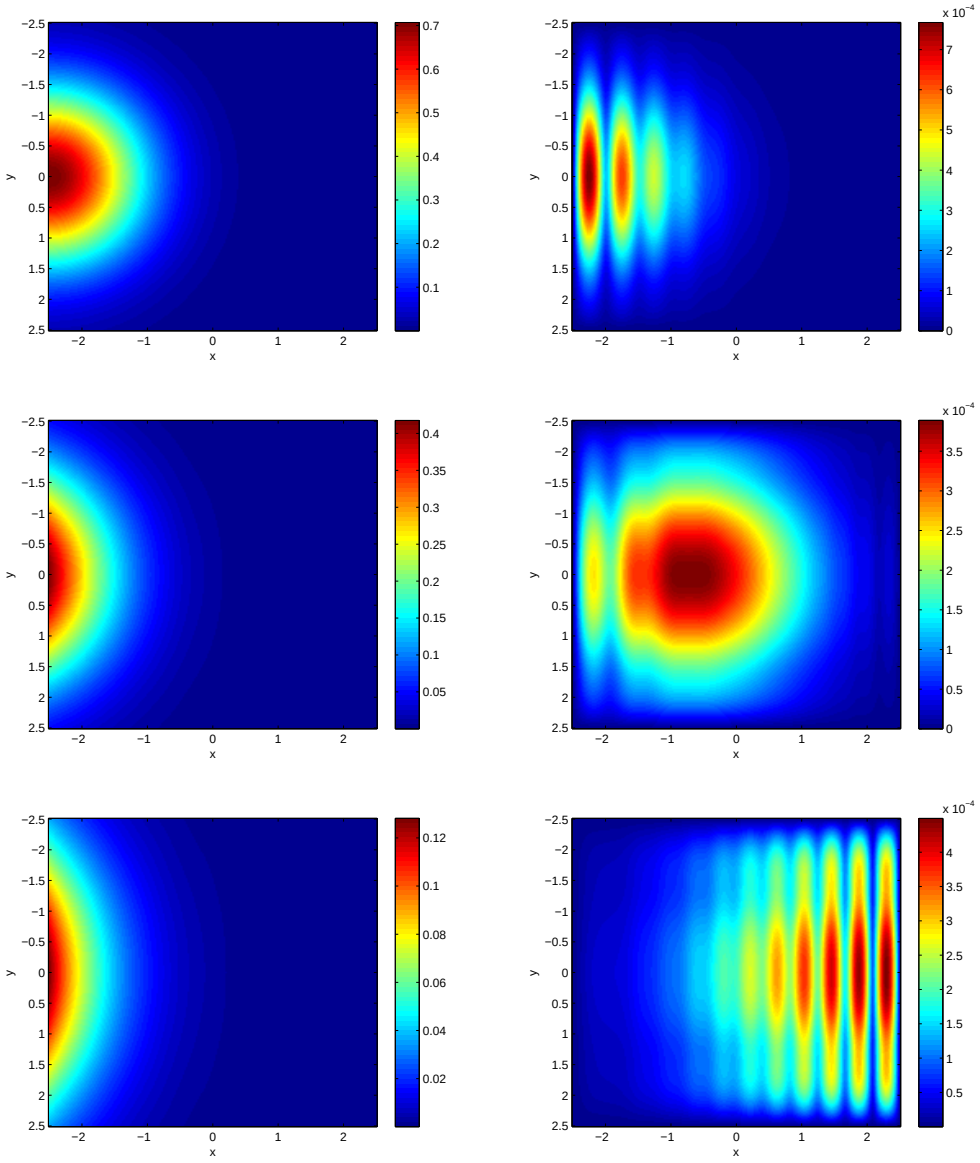

Figure 1: Numerical solutions (left) and absolute errors (right) of the CCD-PRADI method for problem 1 at three time levels $t = 0.25,\ 0.35,\ 0.5$ with $h = \frac{1}{40}$ and $\Delta t = \frac{1}{1000}$.

287.9041 seconds; Nevertheless, in the case that the mesh size is reduced to $\Delta x = \Delta y = \frac{\pi}{16}$, the error of the HOC-ADI method is 6.2142×10^{-6}, which is still greater than the above error of the CCD-PRADI method, while the consumed CPU time is 347.4441 seconds. Hence, in this point of view, the CCD-PRADI method is more efficient than the HOC-ADI method at the same time.

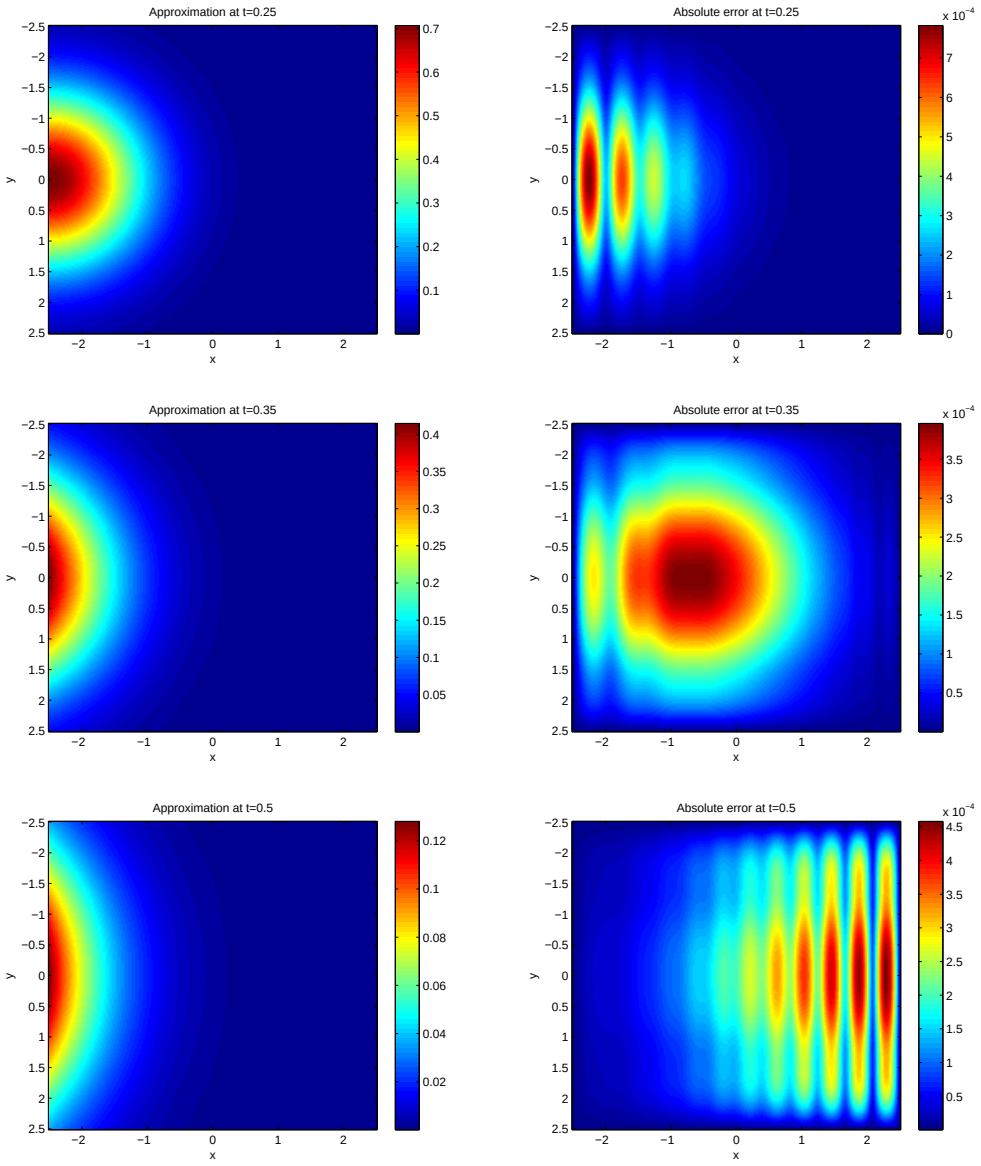

Figure 2: Numerical solutions (left) and absolute errors (right) of the HOC-ADI method for problem 1 at three time levels $t = 0.25,\ 0.35,\ 0.5$ with $h = \frac{1}{40}$ and $\Delta t = \frac{1}{1000}$.

In the CCD-PRADI method, the Picard iteration is applied to tackle the nonlinearity in (11), without proving its convergence. However, it do converge to the exact solution very fast at each step. In this experiment, only two iterations is enough to generate a very accurate approximation at each time level. Fig. 3 shows the fast convergence of the iteration process.

It is worthwhile to note that the Schrödinger equation is mathematically a wave equation,

Table 1: L^2-norm errors and spatial convergence rate at $T = 1$ with $\Delta t = \frac{1}{5000}$.

Δt	h	CCD-PRADI			HOC-ADI		
		Error	Rate	CPU	Error	Rate	CPU
	$\pi/4$	5.1726×10^{-4}	—	80.7474	1.6225×10^{-3}	—	19.8311
$\frac{1}{5000}$	$\pi/8$	4.3040×10^{-6}	6.9090	287.9041	9.9701×10^{-5}	4.0244	80.4126
	$\pi/16$	3.5856×10^{-8}	6.9073	1110.7428	6.2142×10^{-6}	4.0040	347.4441

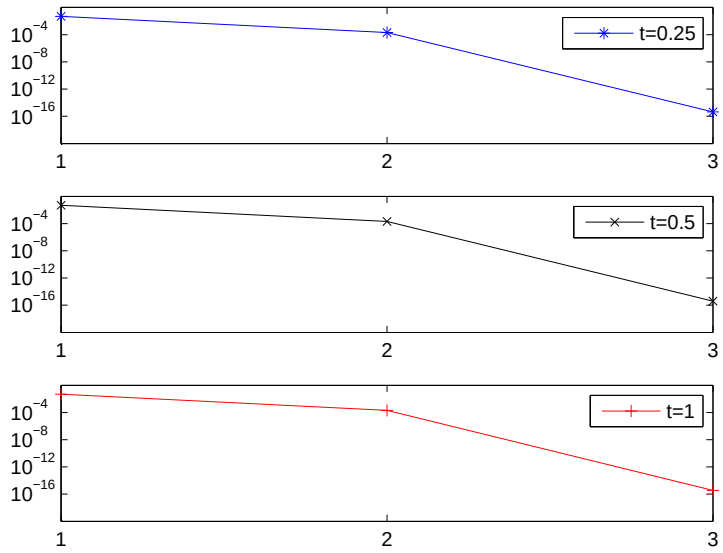

Figure 3: Semilogy plots of maximum error after each iteration at three moments: (a) $t = 0.25$, (b) $t = 0.5$, (c) $t = 1$ with $h = \frac{\pi}{30}$ and $\Delta t = \frac{1}{10000}$.

and the general solutions of wave equations are superpositions of plane waves with some amplitudes, which implying the drifting pattern and periodicity of a solution to a Schrödinger equation. To illustrate the wave-like motion of solution to a Schrödinger equation, surface plots of numerical solutions to *Example 2* by the CCD-PRADI method at three moments, $t = 0.25, 0.5$ and 1, are presented in Fig. 4. And Figs.5 shows the contour plots of numerical solutions to *Example 2* by the CCD-PRADI method and the HOC-ADI method, as well as the analytic solutions at three moments, $t = 0.25, 0.5$ and 1. We can draw a conclusion from Fig. 5 that the CCD-PRADI method is better than the HOC-ADI method to capture the evolution of the solution.

Example 3.

To further illustrate the applicability of the proposed CCD-PRADI method to the two-

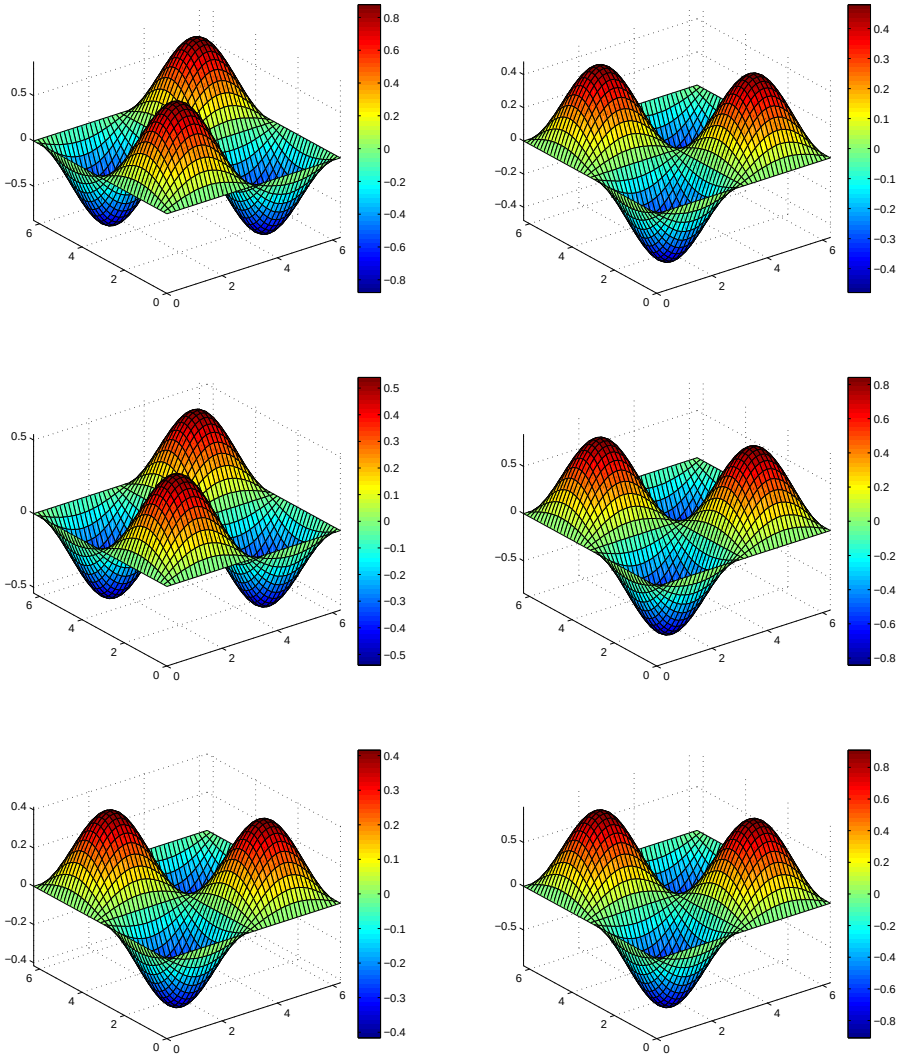

Figure 4: Surface plots of the solution to example 2 at three moments $t = 0.25,\ 0.5,\ 1$ with $h = \frac{\pi}{20}$ and $\Delta t = \frac{1}{5000}$ (left panel and right panel correspond to the real part and the imaginary part of the solution, respectively).

dimensional cubic nonlinear Schrödinger equation of non-homogeneous boundary case, we consider a problem with analytic solution

$$u(x, y, t) = \exp(\mathbf{i}(x + y - t)),$$

which is also used in [24], in the square domain $[0, 2\pi] \times [0, 2\pi]$, and coefficients $q = -1$ and $a = b = \frac{1}{2}$. The Dirichlet boundary condition and initial condition are simply taken from

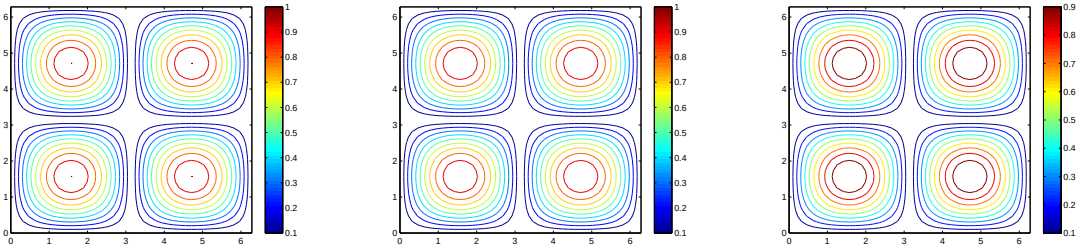

(a) $T = 0.25$

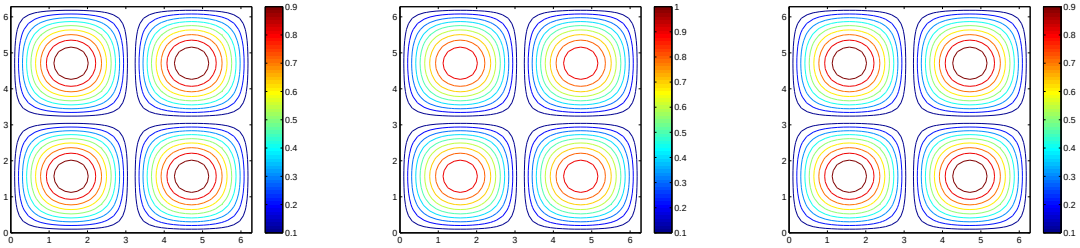

(b) $T = 0.5$

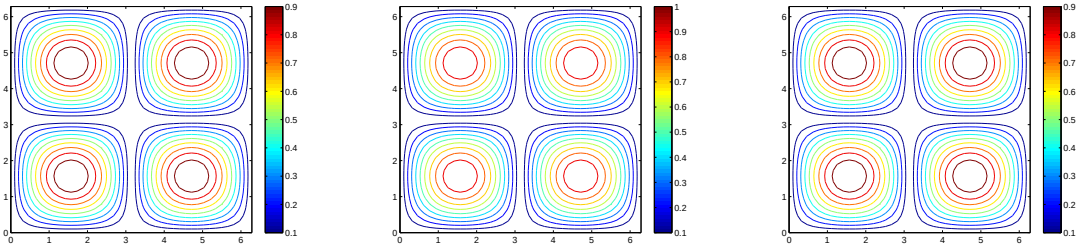

(c) $T = 1$

Figure 5: Contour plots of the modulus of solutions to example 2 at three moments: (a) $t = 0.25$, (b) $t = 0.5$ and (c) $t = 1$ with $h = \frac{\pi}{20}$ and $\Delta t = \frac{1}{5000}$ (left panel, middle panel and right panel correspond to solutions by the CCD-PRADI method, exact solution and solution by the HOC-ADI method, respectively).

the above analytic solution. Since $|u|^2 = 1$, hence the potential function is simply taken as $v(x, y) = -q$.

We present the numerical results in Table 2 to show the temporally second-order accuracy of the CCD-PRADI method under a uniform grid ($\Delta x = \Delta y = \frac{\pi}{64}$). Table 3 further presents the convergence rate of the CCD-PRADI method, as well as the CPU time consumed in the computation. From the results in Table 3, we can conclude that the CCD-PRADI method

is not only more accurate than the HOC-ADI method, but more efficient.

Table 2: L^2-norm errors and temporal convergence rate of the CCD-PRADI method under a uniform grid at $T = 1$.

$\Delta x = \Delta y$	Δt	Error	Rate
$\pi/64$	$T/64$	5.5823×10^{-5}	—
	$T/128$	1.3911×10^{-5}	2.0046
	$T/256$	3.5020×10^{-6}	1.9900
	$T/512$	8.7391×10^{-7}	2.0026

Table 3: L^2-norm errors and spatial convergence rate of the CCD-PRADI method with $\Delta t = 1/25000$ at $T = 1$.

Δt	h	CCD-PRADI			HOC-ADI		
		Error	Rate	CPU	Error	Rate	CPU
$\frac{1}{25000}$	$\pi/4$	3.1146×10^{-4}	—	420.8328	1.1303×10^{-3}	—	100.0178
	$\pi/8$	5.5242×10^{-6}	5.8171	1489.1111	7.3847×10^{-5}	3.9360	412.7028
	$\pi/16$	9.3487×10^{-8}	5.8849	5556.4747	4.7359×10^{-6}	3.9628	1788.3400
	$\pi/32$	1.5356×10^{-9}	5.9279	21824.2260	3.0024×10^{-7}	3.9795	9423.8168

As shown in [24], the solution to *Example 3* is actually a wave function. To further show the "wave-shift" phenomenon of the solution to *Example 3*, surface plots of numerical solutions to *Example 3* by the CCD-PRADI method and the HOC-ADI method at three moments, $t = 0.25, 0.5$ and 1, are presented in Fig. 6 and Fig. 7, respectively. In view of these two figures, we can conclude that the CCD-PRADI method captures the evolution of solution very well.

5. Concluding remarks

In this paper, we developed a CCD-PRADI method for solving two-dimensional cubic NLSEs. The proposed method is sixth-order accurate in space and second-order accurate in time, and unconditionally stable by means of linear stability analysis. Numerical experiments are conducted to test the high order accuracy and efficiency of the CCD-PRADI method and to illustrate the drifting solution pattern of the NLSE.

We remark that the simulation of the vortex dynamics and quantized vortex interactions in the NLSEs and the Ginzburg-Landau-Schrödinger equation (see [2, 3, 27, 28, 1]), has not been considered in this paper, since the proposed method is only for the NLSEs without singularity. It is challenging to exploit the CCD method for those problems and will be our future work.

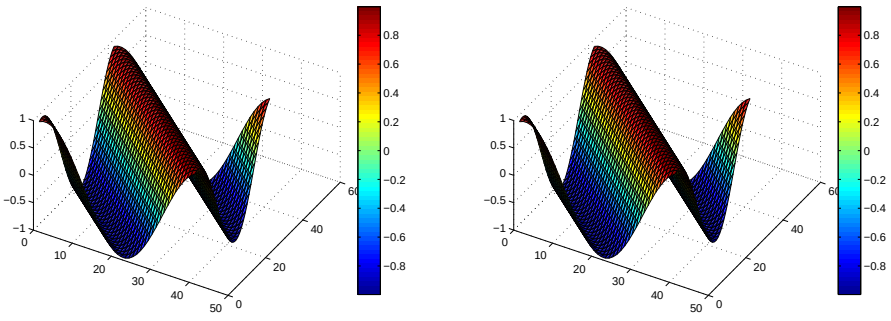

(a)

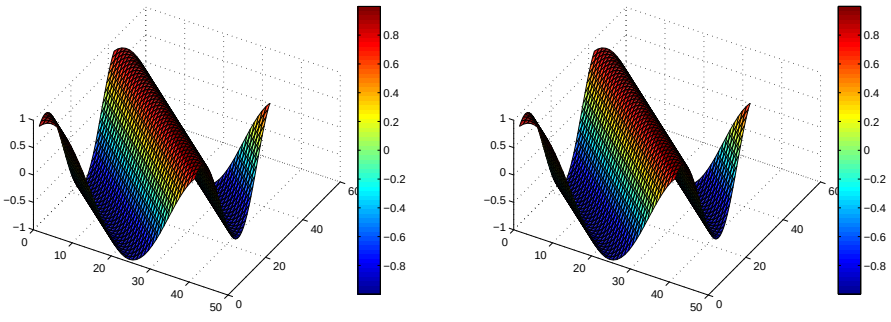

(b)

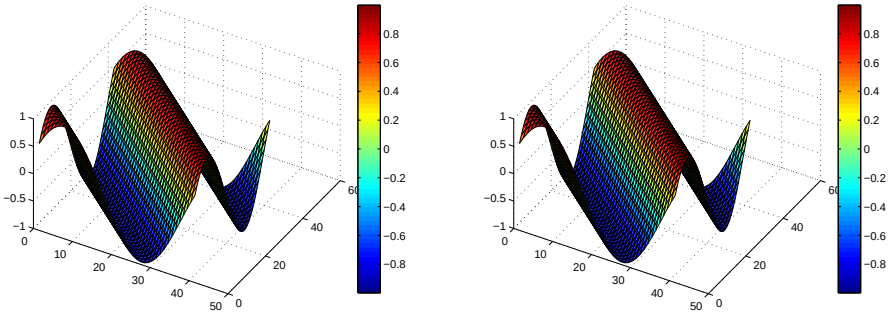

(c)

Figure 6: Surface plots of the real part of solutions to example 3 at three moments: (a) $t = 0.25$, (b) $t = 0.5$ and (c) $t = 1$ with $h = \frac{\pi}{20}$ and $\Delta t = \frac{1}{20000}$ (left panel and right panel correspond to solution by the CCD-PRADI method and exact solution, respectively).

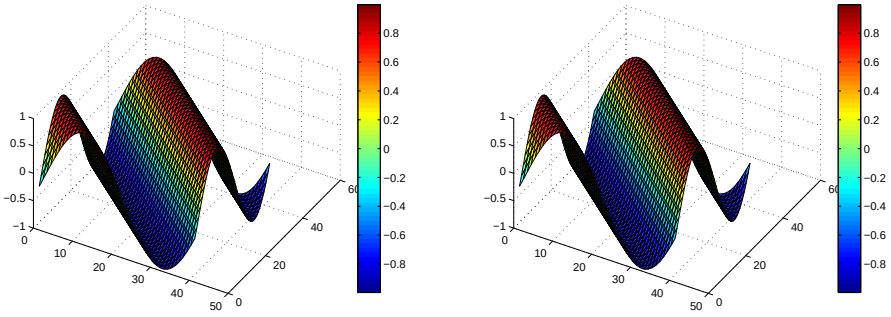

(a)

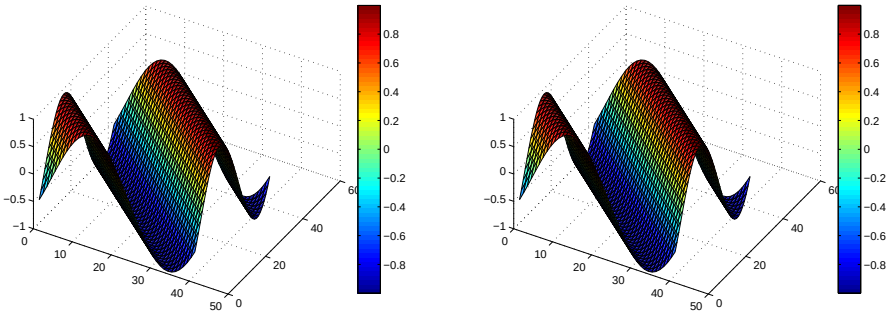

(b)

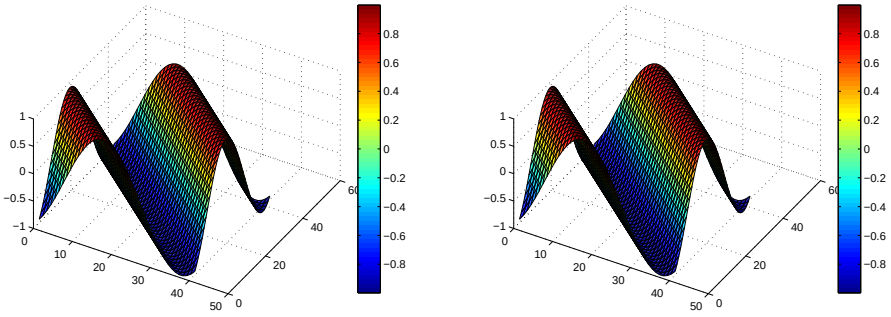

(c)

Figure 7: Surface plots of the imaginary part of solutions to example 3 at three moments: (a) $t = 0.25$, (b) $t = 0.5$ and (c) $t = 1$ with $h = \frac{\pi}{20}$ and $\Delta t = \frac{1}{20000}$ (left panel and right panel correspond to solution by the CCD-PRADI method and exact solution, respectively).

Acknowledgements

We are grateful to Mr. Hoi-Fong Mak for his great help in revising this paper, as well as Dr. Guang-hua Gao for her helpful discussion. We also appreciate two anonymous reviewers for their valuable suggestions which greatly improve the manuscript.

[1] X. Antoine, W. Bao, C. Besse, *Computational methods for the dynamics of the nonlinear Schrödinger/Gross-Pitaevskii equations*, Computer Physics Communications, 184 (2013), pp. 2621–2633.

[2] W. Bao, Y. Cai, *Mathematical theory and numerical methods for Bose-Einstein condensation*, Kinet. Relat. Mod., 6 (2013), pp. 1–135.

[3] W. Bao, Q. Tang, *Numerical study of quantized vortex interaction in nonlinear Schrödinger equation on bounded domain*, Modeling and Simulation: a SIAM Interdisciplinary Journal, 12 (2014), pp. 411–439.

[4] A. G. Bratsos, *A linearized finite difference scheme for the numerical solution of the nonlinear cubic Schrödinger equation*, Korean Journal of Computational and Applied Mathematics, 8 (2001), No. 3, pp. 459–467.

[5] Q. Chang, E. Jia, W. Sun, *Difference schemes for solving the generalized nonlinear Schrödinger equation*, Journal of Computational Physics, 148 (1999), pp. 397–415.

[6] Q. Chang, L. Xu, *A numerical method for a system of generalized nonlinear Schrödinger equations*, J. Comput. Math. 4 (1986), pp. 191–199.

[7] P. Chu, C. Fan, *A three-point combined compact difference scheme*, Journal of Computational Physics, 140 (1998), pp. 370–399.

[8] M. Dehghan, A. Taleei, *A compact split-step finite difference method for solving the nonlinear Schrödinger equations with constant and variable coefficients*, Computer Physics Communications, 181 (2010), pp. 43–51.

[9] L. Erdős, B. Schlein, H. Yau, *Derivation of the cubic non-linear Schrödinger equation from quantum dynamics of many-body systems*, Inventiones mathematicae 167 (2007), pp. 515–614.

[10] G. Fairweather, A. Mitchell, *A new computational procedure for ADI methods*, SIAM J. Numer. Anal., 4 (1967), pp. 163–170.

[11] Z. Gao, S. Xie, *Fourth-order alternating direction implicit compact finite difference schemes for two-dimensional Schrödinger equation*, Applied Numerical Mathematics, 61 (2011) 593–614.

[12] E. Gross, *Structure of a quantized vortex in boson systems*, Nuovo Cimento, 20 (1961), pp. 454.

[13] S. Karaa, J. Zhang, *High order ADI method for solving unsteady convection-diffusion problems*, Journal of Computational Physics, 198 (2004), pp. 1–9.

[14] K. Kirkpatrick, B. Schlein, G. Staffilani, *Derivation of the two-dimensional nonlinear Schrödinger equation from many body quantum dynamics*, American Journal of Mathematics, 133 (2011), pp. 91–130.

[15] M. Lévy, *Parabolic Equation Methods for Electromagnetic Wave Propagations*, IEEE, 2000.

[16] X. Li, L. Zhang, S. Wang, *A compact finite difference scheme for the nonlinear Schrödinger equation with wave operator*, Applied Mathematics and Computation, 219 (2012), pp. 3187–3197.

[17] X. Liu, P. Ding, *Dynamic properties of cubic nonlinear Schrödinger equation with varying nonlinear parameter*, J. Phys. A: Math. Gen, 37 (2004), pp. 1589–1602.

[18] D. Peaceman, H. Rachford, *The numerical solution of parabolic and elliptic differential equations*, Journal of the Society for Industrial and Applied Mathematics, 3 (1955), pp. 28–41.

[19] H. Sun, L. Li, *A CCD-ADI method for unsteady convection-diffusion equations*, Computer Physics Communications, 185 (2014), pp. 790–797.

[20] H. Sun, J. Zhang, *A high-order finite difference discretization strategy based on extrapolation for convection diffusion equations*, Numerical Methods for Partial Differential Equations, 20 (2004), pp. 18–32.

[21] Z. Tian, S. Dai, *High-order compact exponential finite difference methods for convection-diffusion type problems*, Computer Physics Communications, 220 (2007), pp. 952–974.

[22] Z. Tian, Y. Ge, *A fourth-order compact ADI method for solving two-dimensional unsteady convection-diffusion problems*, Journal of Computational and Applied Mathematics, 198 (2007), pp. 268–286.

[23] Z. Tian, P. Yu, *High-order compact ADI (HOC-ADI) method for solving unsteady 2D Schrödinger equation*, Computer Physics Communications, 181 (2010), pp. 861–868.

[24] T. Wang, B. Guo, Q. Xu, *Fourth-order compact and energy conservative difference schemes for the nonlinear Schrödinger equation in two dimensions*, Journal of Computational Physics, 243 (2013), pp. 382–399.

[25] S. Wang, L. Zhang, *Split-step orthogonal spline collocation methods for nonlinear Schrödinger equations in one, two, and three dimensions*, Applied Mathematics and Computation, 218 (2011), pp. 1903–1916.

[26] Y. Xu, L. Zhang, *Alternating direction implicit method for solving two-dimensional cubic nonlinear Schrödinger equation*, Computer Physics Communications, 183 (2012), pp. 1082–1093.

[27] Y. Zhang, W. Bao, Q. Du, *The dynamics and interaction of quantized vortices in Ginzburg-Landau-Schrödinger equations*, SIAM J. Appl. Math., 67 (2007), pp. 1740–1775.

[28] Y. Zhang, W. Bao, Q. Du, *Numerical simulation of vortex dynamics in Ginzburg-Landau-Schrödinger equation*, Eur. J. Appl. Math., 18 (2007), pp. 607–630.

[29] Y. Zhang, Z. Sun, T. Wang, *Convergence analysis of a linearized Crank-Nicolson scheme for the two-dimensional complex Ginzburg-Landau equation*, Numerical Methods for Partial Differential Equations, 29 (2013), pp. 1487–1503.